

Synthesis of Carbon Showing Weak Antiferromagnetic Behavior at a Low Temperature

著者 (英)	Masashi Otaki, Shota Hirokawa, Hiromasa GOTO
journal or publication title	Condensed Matter
volume	4
number	1
page range	33
year	2019-03
権利	(C) 2019 by the authors. Licensee MDPI, Basel, Switzerland. This article is an open access article distributed under the terms and conditions of the Creative Commons Attribution (CC BY) license (http://creativecommons.org/licenses/by/4.0/).
URL	http://hdl.handle.net/2241/00157095

doi: 10.3390/condmat4010033

Communication

Synthesis of Carbon Showing Weak Antiferromagnetic Behavior at a Low Temperature

Masashi Otaki, Shota Hirokawa and Hiromasa Goto * 

Department of Materials Science, Faculty of Pure and Applied Sciences, University of Tsukuba, Tsukuba, Ibaraki 305-8573, Japan; s1720420@s.tsukuba.ac.jp (M.O.); s1720461@s.tsukuba.ac.jp (S.H.)

* Correspondence: gotoh@ims.tsukuba.ac.jp

Received: 31 January 2019; Accepted: 19 March 2019; Published: 21 March 2019



Abstract: In this short communication, we report a new carbon material prepared from *meta*-linked polyaniline that exhibits weak antiferromagnetic interactions at low temperature. The synthesis of poly(*meta*-aniline), abbreviated as *m*-PANI, was conducted using the Ullmann reaction with the aid of Cu^+ as a catalyst in the presence of K_2CO_3 . After the generation of radical cations by vapor-phase doping with iodine, carbonization was performed to prepare carbon polyaniline (C-PANI), which comprises condensed benzene rings. Analysis with a superconducting quantum interference device revealed that the resultant carbon exhibits antiferromagnetism at low temperatures. The discovery of this weak antiferromagnetic carbon may contribute to the development of carbon magnets.

Keywords: polymer magnet; polyaniline; antiferromagnetism; superconducting quantum interference device

1. Introduction

Polymer magnetism has been intensively studied with the aim of obtaining polymer ferromagnets that exhibit a ferromagnetic spin alignment. For example, the magnetic coupling of triplet phenylene units was reported by Iwamura in 1989 [1]; the ferromagnetic behavior of pyrolyzed *o*-, *m*-, and *p*-phenylenediamine and triazine derivatives was reported by Yoshino [2]; and Nishide et al. achieved ferromagnetic spin alignment with 3,4'-bis(diphenylamino)stilbene [3]. Ferromagnetic spin interactions in polymeric aromatic amines have also been reported [4], and, in the field of high-spin polymers, ferromagnetic coupling in hexaazacyclophane units has been reported [5]. Moreover, carbon magnets have been widely studied by both experimental and theoretical techniques [6,7]. Finally, a combination of organic and inorganic materials has been reported to show remarkable stability and a high-spin quartet ground state [8].

Our research group has focused on the development of organic magnetic materials for a long time. Accordingly, in the present study, we synthesized poly(*meta*-aniline) (*m*-PANI) as a carbon precursor, which was subsequently carbonized in an inert atmosphere. The carbon obtained from the polymer exhibits weak low-temperature antiferromagnetism. Although the obtained carbon may exhibit spin interactions with the graphite structure, the full mechanism is currently unclear. In this short report, we present the synthetic method for the preparation of weak antiferromagnetic carbon and the superconducting quantum interference device (SQUID) analysis results as a contribution to the development of carbon magnets.

2. Materials and Methods

2.1. Synthesis

As shown in Figure 1, the Ullmann-type polycondensation between *m*-phenylenediamine and tribromobenzene in nitrobenzene yielded *m*-PANI with a highly cross-linked two-dimensional (2D) structure, according to a previously reported method [9,10]. First, equimolar amounts of *m*-phenylenediamine and tribromobenzene were dissolved in nitrobenzene in the presence of a copper iodide catalyst (see Table 1). The reaction was stirred for 2 days at 200 °C. The resultant black solution was filtered, and the black powder was added to ca. 200 mL of ammonia/water solution to remove the copper. The solution was then filtered again. The filtrate was then added to ca. 200 mL of water and stirred for 24 h. After filtering, the filtrate was added to ca. 200 mL of methanol and stirred for 24 h before filtering again. The black filtrate was dried under reduced pressure. During these processes, care was taken to avoid contamination by Fe and Ni. Subsequently, vapor-phase iodine doping was performed to generate radicals in the *m*-PANI. Then, carbonization of the resultant polymer was performed at 1,000 °C under argon. The resultant material was labeled carbon polyaniline (C-PANI).

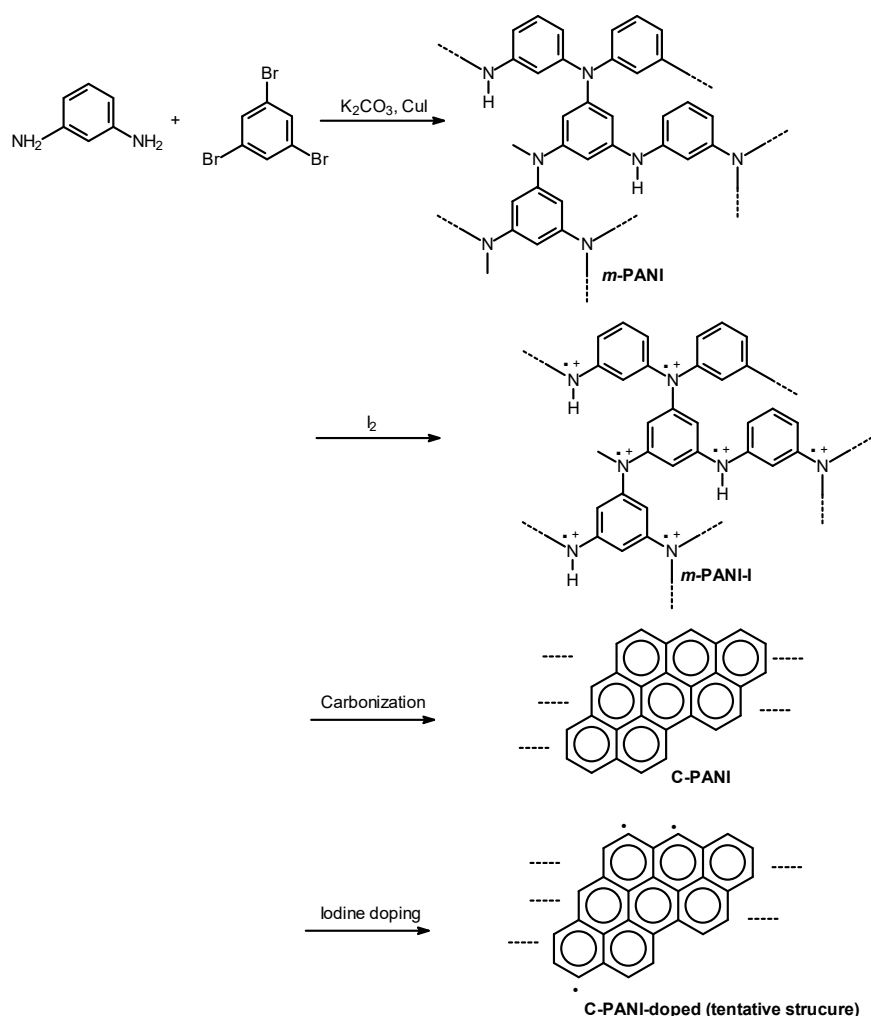
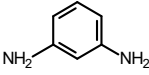
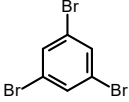
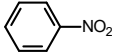


Figure 1. Synthesis of polymers and carbon materials in these studies. All polymer structures are representative. poly(*meta*-aniline) (*m*-PANI): 2D poly(*meta*-aniline) network; *m*-PANI-I: iodine-doped sample containing polarons (radical cations); carbon polyaniline (C-PANI): carbonized sample; C-PANI-doped: carbonized sample with iodine doping.

Table 1. Materials and quantities used for synthesis of poly(*meta*-aniline) (*m*-PANI).

Compound	Role	Chemical Structure	Quantity
<i>m</i> -Phenylenediamine	Monomer		0.12 (g)
Tribromobenzene	Monomer		0.37 (g)
Copper iodide	Catalyst	CuI	0.019 (g)
Potassium carbonate	Co-catalyst	K ₂ CO ₃	0.47 (g)
Nitrobenzene	Solvent		2.35 mL

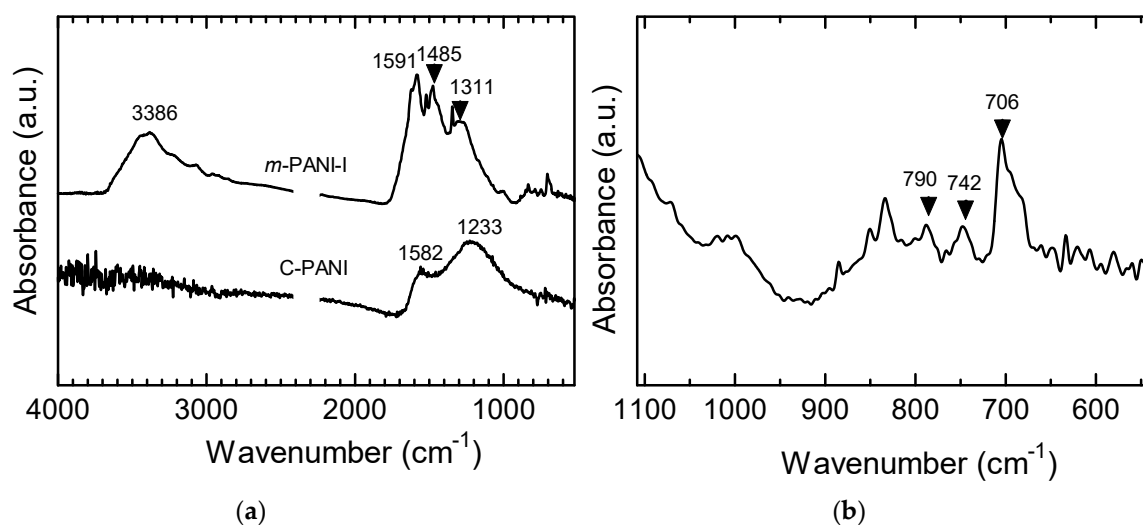
2.2. Instruments

Magnetic susceptibility measurements of the polymer were carried out using a SQUID (Quantum Design CA, Magnetic property measurement system, MPMS). Electron Spin Resonance (ESR) measurements were conducted using a JES TE-200 spectrometer (JEOL, Tokyo, Japan) with 100 kHz modulation (X-band). Infrared (IR) absorption spectra for the polymer samples were obtained with an FT/IR-4600 spectrometer (JASCO, Tokyo, Japan) by the KBr method. Carbonization was carried out with an MIT Lincoln Lab Gold furnace (MIT, Cambridge, MA, USA). Electron Probe Micro Analyzer (EPMA) measurements for the samples were carried with a JEOL JXA-8530F Electron Probe Micro Analyzer (JEOL, Tokyo, Japan).

3. Results

3.1. IR Spectra

Figure 2a shows the IR spectra of *m*-PANI and C-PANI. *m*-PANI presents N-H stretching at 3386 cm⁻¹. The absorption band at 1591 cm⁻¹ is assigned to the C=C stretching of the one-dimensional (1D) quinonoid structures (Figure 2c) in the polymer. The absorption at 1485 cm⁻¹ is due to C=C stretching of the 1D or 2D benzenoid structures in the polymer. Three C-H out-of-plane bending absorptions for the *meta*-linked polymer are observed at 790, 742, and 706 cm⁻¹ (Figure 2b).

**Figure 2.** Cont.

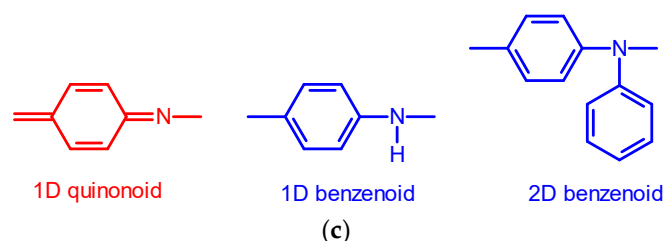


Figure 2. (a) Infrared (IR) absorption spectra of *m*-PANI-I and C-PANI. (b) Magnification of the 1100 to 550 cm^{-1} region of the *m*-PANI-I spectrum. (c) The quinonoid and benzenoid structures in *m*-PANI.

The carbonized sample (C-PANI) shows an absorption band at 1582 cm^{-1} (Figure 2a). This characteristic peak implies partial graphite formation inside the bulk sample. Another prominent peak appears around 1233 cm^{-1} . These results indicate that carbonization affords a graphitic structure. As the carbon has no N-H bonds, no N-H stretching absorptions are observed. Thus, these results confirm that C-PANI, which is a condensed ring structure consisting of benzene, is formed by the complete carbonization of *m*-PANI-I. Figure 1 (bottom) shows a plausible structure of the carbon comprising benzene structures.

Figure 3 displays Electron probe micro analyzer (EPMA) results for *m*-PANI (a) and C-PANI (b). *m*-PANI as a sample of before carbonization consists of C, N, and O. However, C-PANI, as a carbonized sample, has no nitrogen atom, indicating that the sample after carbonization has no pyridinic structure.

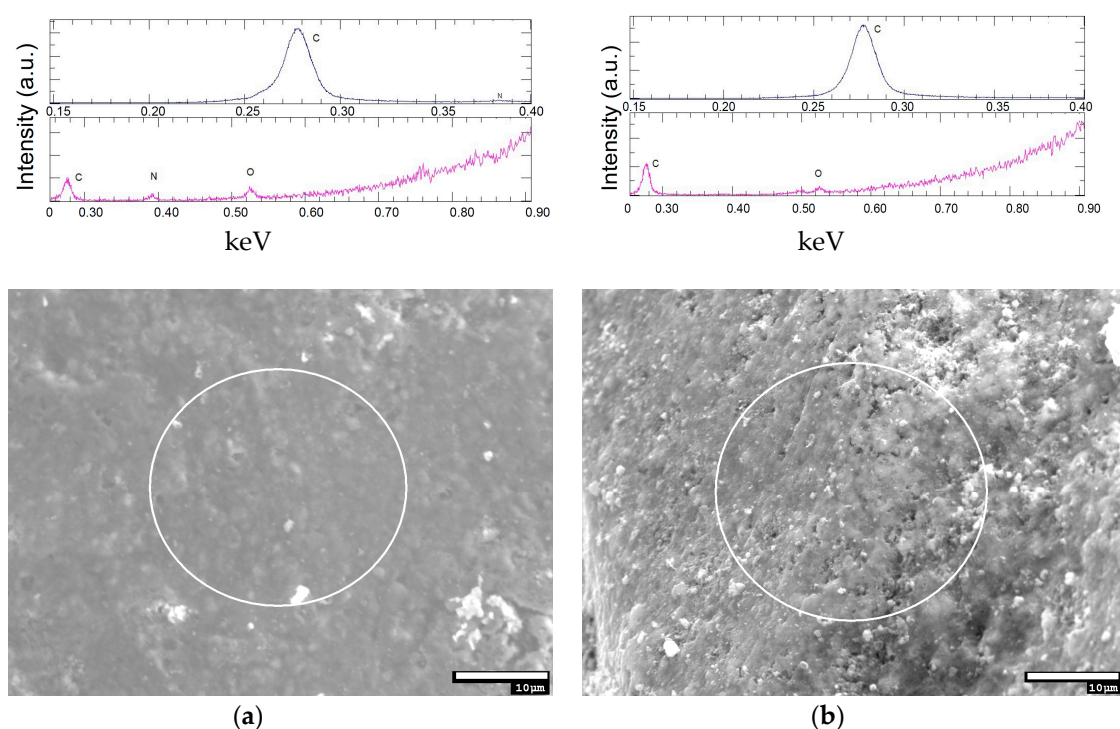


Figure 3. Electron probe micro analyzer (EPMA) results for *m*-PANI (a) and C-PANI (b). Scale bar = 10 μm . Top: signals from atoms. Bottom: Scanning electron microscopy (SEM) images.

3.2. Magnetic Measurement

Figure 4 shows the ESR trace measured at $24\text{ }^\circ\text{C}$ for *m*-PANI after iodine doping. Data points are 4096 in this measurement. Lorentz-type symmetric absorption is observed due to the radical cations on the N atoms. This demonstrates that the polymer has paramagnetic characteristics.

Figure 5 shows results of SQUID magnetometry measurements for C-PANI. The magnetic susceptibility (χ) of C-PANI increases as the temperature decreases. The plot of $1/\chi$ vs. T presents

a linear decrease. This indicates that the Weiss temperature of C-PANI is -0.3 K due to weak antiferromagnetic behavior at a low temperature. The values of χT in the Curie plot for C-PANI decrease at a low temperature. This result confirms that C-PANI is antiferromagnetic.

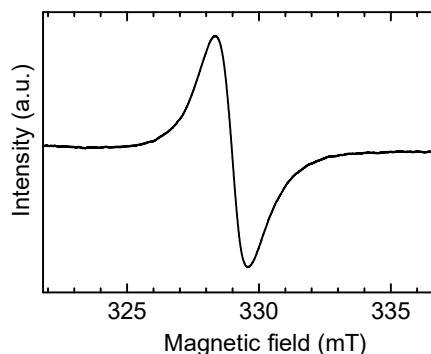


Figure 4. Electron Spin Resonance (ESR) trace for *m*-PANI after vapor-phase iodine doping.

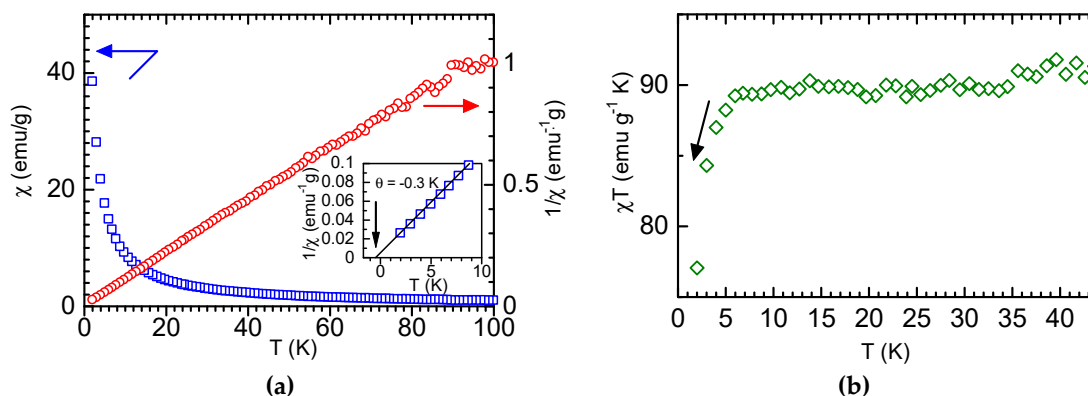


Figure 5. Superconducting quantum interference device (SQUID) magnetometry results for C-PANI. (a) χ vs. T and $1/\chi$ vs. T . (b) χT vs. T as Curie plots.

Finally, we investigated the magnetic properties of the iodine-doped carbon prepared from *m*-PANI, labeled C-PANI-doped. C-PANI was dried in vacuo to remove oxygen before iodine doping. The χ value for C-PANI-doped increases as the temperature decreases, and the maximum is observed at ca. 43 K. In $1/\chi$ vs. T plots, C-PANI-doped shows a linear decrease to 66 K upon cooling (Figure 6a). χT increases upon cooling to 44.6 K and decreases thereafter to 0 K (Figure 6b). Figure 7 displays the occurrence of a linear regime as Ising 1D systems [11–13]. The χT vs T^{-1} plot increases linearly (dashed line). The experimental data indicate a ferromagnetic coupling.

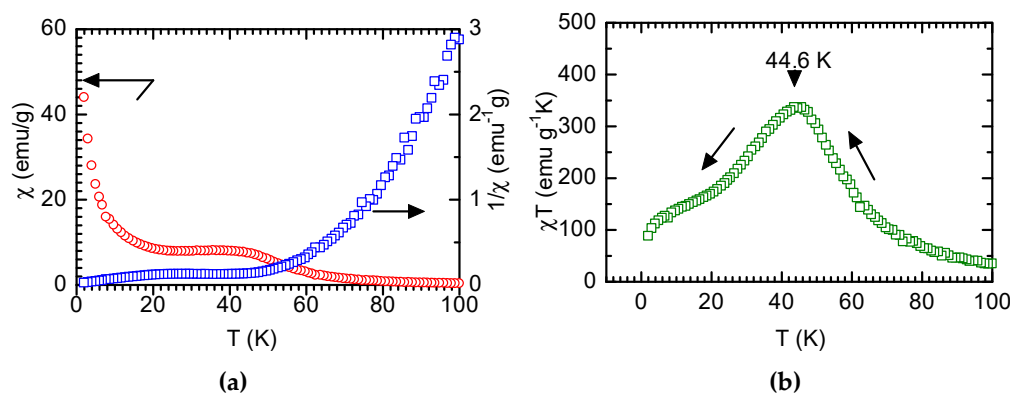


Figure 6. SQUID magnetometry results for C-PANI-doped. (a) χ vs. T and $1/\chi$ vs. T . (b) χT vs. T as Curie plots.

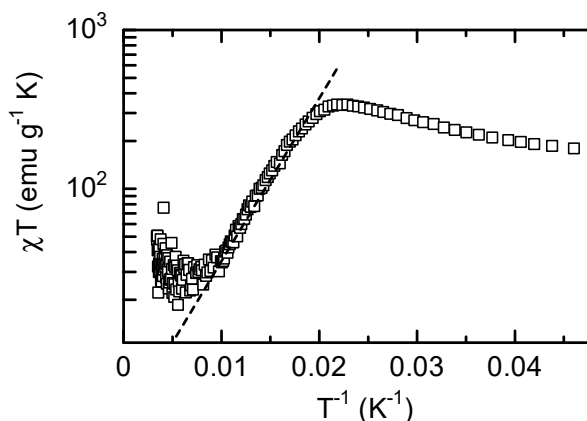


Figure 7. Ining plots for C-PANI-doped.

Even though high-vacuum treatment of the sample was performed before doping, the possibility of residual oxygen in the sample may need to be considered further. Radical cations of the graphite structure produced by iodine doping may interact by spin alignment to show partial ferromagnetic-like behavior.

4. Discussion

m-PANI was prepared by the Ullmann polycondensation using Cu^+ [9,10]. This reaction affords a 2D-structured polymer constructed with amine linkages. Subsequent vapor-phase iodine doping generates radicals. Radical generation in the polymer induces good carbonization activity. Carbonization under argon yields a black powder. The resultant C-PANI contains graphite structures. This carbon contains random defects in its graphite structure, which may exhibit antiferromagnetic order. In this short communication, we have reported a new carbon prepared from *m*-PANI, which exhibits weak antiferromagnetic interactions at low temperature. The *meta*-linkages in *m*-PANI may be related to its high-spin state [14]. The *meta*-form of the precursor *m*-PANI used in this study may endow a certain spin structure onto the resultant carbon. The structural and chemical dynamics in graphene play a central role in magnetic functionality [15]. Iodine doping may produce ferromagnetic-like interactions in the carbon sample. However, the reason for these interactions is unclear at the present time.

Author Contributions: H.G. carried out synthesis of the polymers. S.H. conducted carbonization. M.O. measured IR, EPMA, ESR and SQUID; M.O. and H.G. contributed the data analysis; M.O. and H.G. discussed the results and wrote the final version of the manuscript; All authors have read and approved the final manuscript.

Funding: This research received no external funding.

Acknowledgments: We would like to thank the OPEN FACILITY, Research Facility Center for Science and Technology, University of Tsukuba for using EPMA and Glass Work Shop of University of Tsukuba.

Conflicts of Interest: The authors declare no conflict of interest.

References

- Iwamura, H.; Murata, S. Magnetic coupling of two triplet phenylnitrene units joined through an acetylenic or a di-acetylenic linkage. *Mol. Cryst. Liq. Cryst. Incorpor. Nonlinear Opt.* **1989**, *176*, 33–47. [[CrossRef](#)]
- Araki, H.; Matsuoka, R.; Yoshino, K. Ferromagnetic behavior of pyrolyzed o,m,p-phenylenediamine and triazine derivatives. *Solid State Commun.* **1991**, *79*, 443–446. [[CrossRef](#)]
- Michinobu, T.; Takahashi, M.; Tsuchida, E.; Nishide, H. Robust Triplet Molecule: Cationic Diradical of 3,4'-Bis(diphenylamino)stilbene. *Chem. Mater.* **1999**, *11*, 1969–1971. [[CrossRef](#)]
- Dobrzyńska, E.; Jouni, M.; Gawryś, P.; Gambarelli, S.; Mouesca, J.-M.; Djurado, D.; Dubois, L.; Wielgus, I.; Maurel, V.; Kulszewicz-Bajer, I. Tuning of ferromagnetic spin interactions in polymeric aromatic amines via modification of their π -conjugated system. *J. Phys. Chem. B.* **2012**, *116*, 14968–14978. [[CrossRef](#)] [[PubMed](#)]

5. Skorka, L.; Kurzep, P.; Chauviré, T.; Dubois, L.; Mouesca, J.-M.; Maurel, V.; Kulszewicz-Bajer, I. High-spin polymers: ferromagnetic coupling of $s = 1$ hexaazacyclophane units up to a pure $s = 2$ polycyclophane. *J. Phys. Chem. B* **2017**, *121*, 4293–4298. [[CrossRef](#)] [[PubMed](#)]
6. Yang, X.; Xia, H.; Qin, X.; Li, W.; Dai, Y.; Liu, X.; Zhao, M.; Xia, Y.; Yan, S.; Wang, B. Correlation between the vacancy defects and ferromagnetism in graphite. *Carbon* **2009**, *47*, 1399–1406. [[CrossRef](#)]
7. Ali, M.; Pi, X.; Liu, Y.; Yang, D. Electronic and magnetic properties of graphene, silicone and germanene with varying vacancy concentration. *AIP Adv.* **2017**, *7*, 045308. [[CrossRef](#)]
8. Shimizu, D.; Osuka, A. A benzene-1,3,5-triaminyl radical fused with Zn^{II} -porphyrins: remarkable stability and a high-spin quartet ground state. *Angew. Chem. Int. Ed.* **2018**, *57*, 3733–3736. [[CrossRef](#)] [[PubMed](#)]
9. Ullmann, F.; Bielecki, J. Synthesis in the biphenyl series. *Ber. Dtsch. Chem.* **1901**, *34*, 2174. [[CrossRef](#)]
10. Yoshizawa, K.; Tanaka, K.; Yamabe, T.; Yamauchi, J. Ferromagnetic interaction in poly(m-aniline): Electron spin resonance and magnetic susceptibility. *J. Chem. Phys.* **1992**, *96*, 5516–5522. [[CrossRef](#)]
11. Mougél, V.; Chatelain, L.; Hermle, J.; Caciuffo, R.; Colineau, E.; Tuna, F.; Magnani, N.; de Geyer, A.; Pécaut, J.; Mazzanti, M. A Uranium-based $UO_2^{+}-Mn^{2+}$ single-chain magnet assembled through cation–cation Interactions. *Angew. Chem. Int. Ed.* **2014**, *53*, 819–823. [[CrossRef](#)] [[PubMed](#)]
12. Coulon, C.; Clerac, R.; Lecren, L.; Wernsdorfer, W.; Miyasaka, H. Glauber dynamics in a single-chain magnet: From theory to real systems. *Phys. Rev. B.* **2004**, *69*, 132408. [[CrossRef](#)]
13. Zhang, W.-X.; Ishikawa, R.; Breedlove, B.; Yamashita, M. Single-chain magnets: Beyond the Glauber model. *RSC Adv.* **2013**, *3*, 3772–3798. [[CrossRef](#)]
14. Gałecka, M.; Wielgus, I.; Zagórska, M.; Pawłowski, M.; Kulszewicz-Bajer, I. High-spin radical cations of poly(*m-p*-anilines) and poly(*m-p-p*-anilines): Synthesis and spectroscopic properties. *Macromolecules* **2007**, *40*, 4924–4932. [[CrossRef](#)]
15. Lin, Y.-C.; Teng, P.-Y.; Yeh, C.-H.; Koshino, M.; Chiu, P.-W.; Suenaga, K. Structural and chemical dynamics of pyridinic-nitrogen defects in graphene. *Nano Lett.* **2015**, *15*, 7408–7413. [[CrossRef](#)] [[PubMed](#)]



© 2019 by the authors. Licensee MDPI, Basel, Switzerland. This article is an open access article distributed under the terms and conditions of the Creative Commons Attribution (CC BY) license (<http://creativecommons.org/licenses/by/4.0/>).